Available online at www.sciencedirect.com
SCIENCE DIRECT®
Applied Surface Science 223 (2004) 138–143
applied surface science
www.elsevier.com/locate/apsusc

The properties of cadmium tin oxide thin-film compounds prepared by linear combinatorial synthesis

Xiaonan Li*, Timothy A. Gessert, Timothy Coutts

National Renewable Energy Laboratory, 1617 Cole Blvd., Golden, CO 80401, USA

Abstract

SnO_2 and CdO films with high electrical and optical quality have been produced by using low-pressure metal-organic chemical vapor deposition. Based on the knowledge gained from binary oxide formation, linear combinatorial synthesis is used to study the ternary oxide (Cd–Sn–O) compound. Compositional, structural, electrical, and optical properties of the films are found to vary along the reactant gas flow direction. The crystal structure indicates that the CdO-like films are formed near the location of gas injection and SnO_2-like films near the end of the deposition zone. As composition and structure change, the carrier concentration varies around 10^{20} cm^{-3}, and the mobility increases from less than 1 to ~60 cm^2 V^{-1} s^{-1}. The optical bandgap of the films also increases from ~2.75 to 3.65 eV as composition moves from CdO-like films to SnO_2-like films.

PACS: 61.10.kw; 78.66.Sq; 81.05.Je

Keywords: Thin film; Transparent conducting oxides; Cadmium tin oxide; MOCVD; Linear combinatorial synthesis; Material properties

1. Introduction

Transparent conducting oxides (TCOs) are used extensively for a variety of applications, including architectural windows, flat-panel displays, thin-film photovoltaics, electrochromic windows, and polymer-based electronics [1]. Some of these applications constitute a large market, attesting to the great commercial importance of TCOs [2]. Owing to their electrical, optical, mechanical, and chemical-resistance properties, conductive SnO_2 films on glass substrates are used extensively for low-emissivity windows for energy conservation and for thin-film photovoltaic solar cells. The quantity of energy-efficient architectural glass produced annually reaches tens of square kilometers, and the market continues to grow. In comparison, CdO is not a popular TCO material due to its narrow optical bandgap of 2.28 eV. However, it has demonstrated electron mobility 5–10 times greater than commercially available TCOs.

Cd_2SnO_4, the ternary TCO material, combines many beneficial characteristics of both SnO_2 and CdO. It is an n-type semiconductor with either orthorhombic or spinel crystal structure. Thin-film Cd_2SnO_4 has demonstrated electron mobility up to 65 cm^2 V^{-1} s^{-1}, high

* Corresponding author. Present address: National Renewable Energy Laboratory, 1617 Cole Blvd., Golden, CO 80401, USA. Tel.: +1-303-384-6428; fax: +1-303-384-6430.
E-mail address: xiaonan_li@nrel.gov (X. Li).

0169-4332/$ – see front matter © 2003 Published by Elsevier B.V.
doi:10.1016/S0169-4332(03)00909-7

electrical conductivity, and low visible absorption. These properties make it potentially suitable for a wide range of applications [3–7]. Unfortunately, the processes that have been used to produce high-quality Cd_2SnO_4—rf sputtering and high-temperature proximity heat treatment—are likely not suitable for large-volume manufacture. Chemical vapor deposition (CVD) is a thin-film deposition technique that has produced high-quality films in a variety of different material systems. It is easily scaled and widely used by industry. In this paper, we review the use of CVD techniques to produce high-quality SnO_2 and CdO films. The knowledge gained from the binary materials is used to study Cd–Sn–O thin-film compounds.

2. Experimental

SnO_2, CdO, and Cd–Sn–O films were fabricated using a low-pressure CVD system made by CVD Equipment Co. (Ronkonkoma, NY). Ultrahigh-purity tetramethyltin (TMT, Morton International) and dimethylcadmium (DMCd, Morton International) were used for the Sn and Cd precursors. UHP-grade oxygen was used for the oxidizer, and nitrogen carrier gas was supplied from a cryogenic source. The nitrogen carrier gas, precursors, and oxygen were mixed before being introduced into the deposition chamber via two gas injectors located on the top and bottom of a stainless steel, chamber-endcap flange.

The reaction chamber was a cold-walled, rectangular quartz tube. Fig. 1 shows the schematic top view. The reactant gas flow direction was defined as the *x*-axis, and the cross gas flow direction, along the sample surface, was defined as the *y*-axis. The reactant gases entered at one end of the chamber, flowed along the chamber length (*x*-axis), and were pumped out from the other end. This deposition configuration allowed us to achieve a linear combinatorial synthesis. Chamber pressure, during the deposition, was maintained between 20 and 80 Torr. Samples were arranged horizontally on a graphite susceptor with a sample pocket 1 mm deep, 102 mm wide, and 306 mm long. The substrates used in this study were Corning 7059 borosilicate glass, 1 mm thick, and 102 mm × 102 mm in area. The graphite susceptor was heated by five-zone infrared lamps. These lamps are independently controlled, along *x*-axis arranged, and located beneath the reaction chamber.

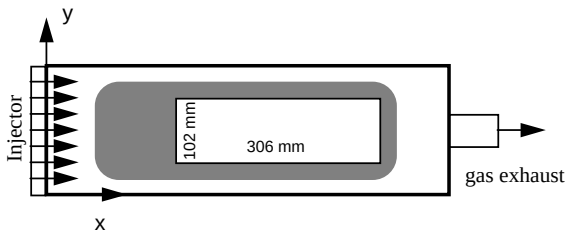

Fig. 1. Schematic top view of MOCVD reactor used to fabricate the TCO samples.

The composition of the films was analyzed by electron-probe microanalysis (EPMA, JEOL 8900 Electron Microprobe), and crystal properties were assessed by X-ray diffraction (XRD, Sintag Model PTS). A Cary 5G spectrophotometer with an integrating-sphere detector and a helium–neon light was used to measure the total transmittance (*T*) and reflectance (*R*) spectrum in the wavelength range of 200–2000 nm. A stylus profilometer (Dektak^3) was used to measure the film thickness. The carrier concentration and electron mobility were measured by Hall measurements (van der Pauw technique, BioRad Model HL5500).

3. Results and discussion

3.1. CVD-formed SnO_2 thin films

We studied the widely used SnO_2 film, both intrinsic and F-doped, by using low-pressure metal-organic chemical vapor deposition (LP-MOCVD). Tetramethyltin (TMT) and bromotrifluoromethane ($CBrF_3$) were tin and fluorine precursors, respectively. The studies indicated that the TMT chemistry yields films with higher transparency and conductivity compared to films produced using a chlorine-containing precursor. A brief review of results from the studies follows.

The MOCVD-formed SnO_2 was a polycrystalline thin film with a tetragonal crystal structure. The growth temperatures were in the range of about 500–700 °C. Below 500 °C, the film deposition rate was extremely low; above 500 °C, the film deposition rate was in the range of 40–400 nm/min. XRD measurements indicated that for SnO_2 films deposited at

500 °C, a good crystallization with a (2 0 0) preferred orientation was formed. As growth temperature increased, the film crystallization, grain size, and surface roughness increased. Once growth temperature rose to close to 700 °C, the density of SnO_2 nuclei was reduced to a level where a discontinuous film formed. Therefore, the deposition temperature in the range of 500–550 °C was used to make continuous and smooth films.

Intrinsic SnO_2 films (i-SnO_2) are weakly n-type due to deviations from stoichiometry. The carrier concentration of F-doped SnO_2 increases from low-10^{18} cm^{-3} to mid-10^{20} cm^{-3} with fluorine partial pressure. Increasing the F-doping level not only increased the carrier concentration, but also increased the electron mobility (μ). Therefore, increasing both the carrier concentration and mobility reduced the resistivity of SnO_2:F film from $\sim$1 Ω cm for undoped material to $\sim 5 \times 10^{-4}$ Ω cm for optimum doping.

The optical properties of MOCVD-fabricated SnO_2 were very high. The optical absorption edge of the films calculated from transmittance and reflectance data was around 3.8 eV. In the visible spectral range, the average optical transmittance for $\sim$0.5 μm-thick SnO_2 films with 7059 glass was larger than 80%, with absorbance of about 5%. The F-doped SnO_2 films had slightly higher sub-bandgap optical absorption than the undoped films. The average absorption coefficients of 500–900 nm wavelength for undoped SnO_2 films were about half the value for F-doped SnO_2 films.

3.2. CVD-formed CdO thin films

CdO is an n-type semiconductor with a bandgap of 2.28 eV, which is smaller than SnO_2 (3.6 eV). CdO thin films have been deposited using reactive sputtering, spray pyrolysis, and activated reactive evaporation [8–14]. Our group was among the first to report on depositing CdO thin films by MOCVD [15].

The CdO films formed by MOCVD are polycrystalline with cubic structure. Within the studied temperature range (100–450 °C), the film crystal structure was very sensitive to growth temperature. At growth temperatures below 250 °C, the film crystallization was poor. At growth temperatures above 300 °C, the CdO films became strongly crystallized with a preferred (2 0 0) orientation. When the growth temperatures reached above 400 °C, large grains formed and the film became discontinuous. The intra-grain quality improved with increasing temperature [16]. Thus, a high Hall mobility was reached in samples formed by high temperature.

For undoped films, the carrier concentration varied systematically with deposition temperature. At a very low growth temperature (100 °C), electron mobility was low ($\sim$1 cm^2 V^{-1} s^{-1}), but the carrier concentration was very high, approaching 2×10^{21} cm^{-3}. As deposition temperature increased to 450 °C, electron mobility increased to values exceeding 200 cm^2 V^{-1} s^{-1}, and the carrier concentration decreased [16]. A Hall mobility of 260 cm^2 V^{-1} s^{-1} was observed on a CdO film deposited at a substrate temperature of 450 °C with fluorine doping. This mobility value was substantially greater than those reported for films formed by other techniques and even for bulk material [17].

In general, the sub-bandgap optical transmission of MOCVD-formed CdO films is lower than SnO_2 film. Depending on the film growth temperature and film thickness, the transmission varied from 60–85%. The color of films also varied with growth temperature. For those films deposited at low temperature, the color was light yellow, whereas for films deposited at higher temperatures, the color was light orange. This color change indicated that the fundamental optical absorption edge shifted as deposition temperature varied. We observed that the bandgap of CdO increased from 2.3–3.3 eV as deposition temperature decreased and carrier concentration increased.

3.3. CVD-formed cadmium-tin-oxide thin films

Cd_2SnO_4 is a transparent conducting oxide that has high electron mobility. Nozik was the first researcher to report a high Hall mobility in thin-film Cd_2SnO_4 produced by rf sputtering [3]. The mobility achieved was as high as 100 cm^2 V^{-1} s^{-1}, with a carrier concentration of 5×10^{18} cm^{-3}. Later, Haacke reported that by using substrate bias or a post-deposition heat treatment in a CdS/Ar atmosphere, one could minimize the extent of the CdO phase and increase carrier concentration [18]. In our laboratory, rf magnetron sputtering with post-deposition heat treatment had also been used to fabricate Cd_2SnO_4 films having high carrier concentration and low optical absorption

[19]. Besides rf sputtering, various deposition methods, such as dc reactive sputtering, ion beam sputtering, spray pyrolysis, and electroless deposition were also used to prepare cadmium stannate thin films [18]. However, to our knowledge, the use of CVD to form Cd_2SnO_4 had not been reported.

In this study, a MOCVD-formed Cd–Sn–O compound was studied. The knowledge gained in forming SnO_2 and CdO films was used to design the experiment. TMT and DMCd metal-organic precursors had different decomposition temperatures; therefore, at a given growth temperature, the decomposition rates of Sn and Cd precursors were different. As reactant gas flowed along the *x*-axis, the precursor that had a high decomposition rate would deplete quicker than the one having a lower decomposition rate. Thus, the concentrations of the Sn and Cd precursors would change along the *x*-axis, causing the composition of the Cd–Sn–O compound to vary along the *x*-axis. With this configuration, by varying the deposition parameters such as temperature and precursor ratio, we were able to form linear combinatorial synthesis libraries. The libraries covered almost the whole composition range of the SnO_2–CdO system. Details will be discussed in the following section.

First, EPMA was used to characterize the changes in film composition. The results indicated that the composition along the *y*-axis (across the gas-flow direction) was fairly uniform. Only on the edge, within a 10–15 mm zone, did the composition vary. Thus, the EPMA data used in the following analysis were taken from off-edge area. Fig. 2 shows an EPMA compositional analysis on one of the Cd–Sn–O samples (CTO62) along the *x*-axis. The precursor ratio—TMT to DMCd—used for this growth was equal to 1.2. The growth temperature was 500 °C at the leading edge of the substrate and increased to 550 °C at the trailing edge. At this deposition temperature range, the decomposition rate of DMCd was much higher than that of TMT; thus, a CdO-like film should be formed at the leading edge of the substrate. As reactant gas flowed along the *x*-axis, the DMCd precursor depleted much more quickly than TMT; thus, the Cd in the film should be decreased. EPMA results indicate that on the leading edge of the substrate, the ratio of Cd to Cd + Sn is 0.75, whereas on the trailing edge, the ratio becomes 0.5. The film composition changed from CdO-like to more $CdSnO_3$-like material.

Along with composition analysis, the structural, electronic, and optical properties were also characterized. Fig. 3 shows a group of XRD spectra taken

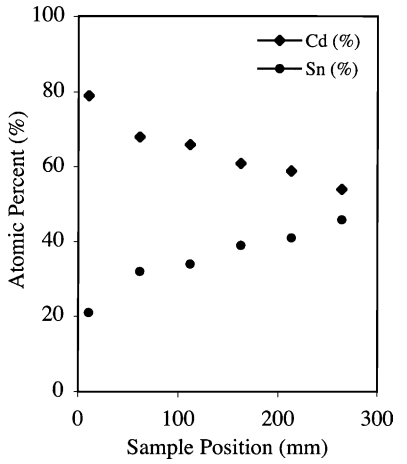

Fig. 2. EPMA composition analysis of a Cd–Sn–O sample (CTO62). The data are taken from different sample positions along the reactant gas-flow direction. Position 0 is on the leading edge of the substrate.

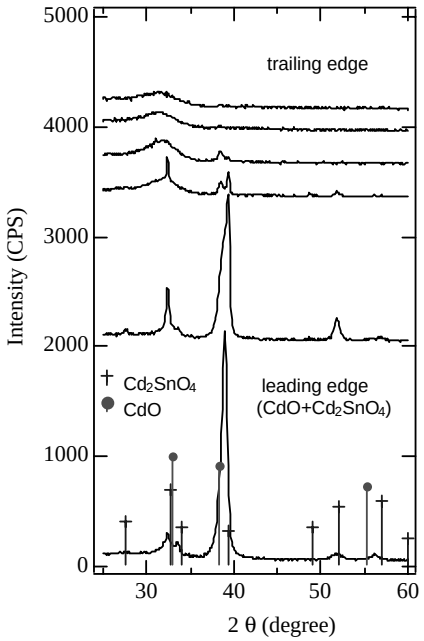

Fig. 3. XRD spectra taken from sample CTO62. Cubic CdO and spinel Cd_2SnO_4 spectra are observed on the leading edge of the substrate, and amorphous spectra are observed on the trailing edge.

from sample CTO62. The crystal structures of cubic (CdO) and cubic spinel (Cd_2SnO_4) are observed clearly in the leading edge of the sample. As the sampling location moves toward the trailing edge, the CdO cubic spectrum disappears first, then the Cd_2SnO_4 spectrum disappears. Finally, the films become amorphous in structure. Composition analysis indicated that in the amorphous area, the Sn and Cd composition is nearly equal. However, no $CdSnO_3$ phase was observed.

As film compositional and structural properties changed along the *x*-axis, the electronic properties of the films also changed. Fig. 4 shows that, for sample CTO62, as composition varied, the carrier concentration also varied from a high $10^{20}\,cm^{-3}$ level at the leading edge to a low $10^{20}\,cm^{-3}$ level at the trailing edge. Whereas the carrier concentration decreased, the Hall mobility increased from less than 20 to $\sim 50\,cm^2\,V^{-1}\,s^{-1}$. Consequently, the resistivity of the films varied from 5×10^{-4} to $11 \times 10^{-4}\,\Omega\,cm$. Note that in this study, a higher Hall mobility was always observed in the amorphous area. A more detailed structural and compositional analysis is ongoing to understand the cause of high mobility in the amorphous region.

The optical properties of the films were characterized by spectrophotometry. The optical bandgap of Cd–Sn–O compounds were calculated from transmittance and reflectance data. In general, the Cd–Sn–O film is light yellow in color when it is Cd rich and colorless, as it becomes Sn rich. The sub-bandgap transmittance of Cd–Sn–O films with glass substrates is around 80–90%. Bandgaps in a wide range were obtained for the Cd–Sn–O compounds. The narrowest band gap of 2.35 eV (characteristic of CdO) and the widest of 3.65 eV (characteristic of SnO_2) was observed on the leading edge and trailing edge of sample, respectively. Fig. 5 shows the transmittance spectra taken from sample CTO62. The calculation from Fig. 5 indicated that the optical bandgap is 2.35 eV on the leading edge, and is ~3.3 eV on the trailing edge.

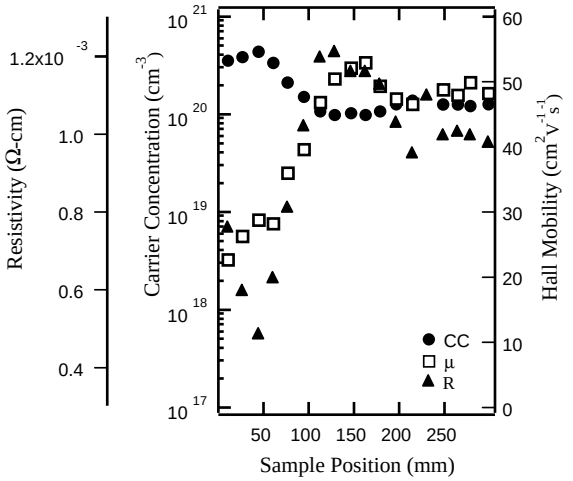

Fig. 4. Electrical properties of CTO62 are plotted as a function of sample position.

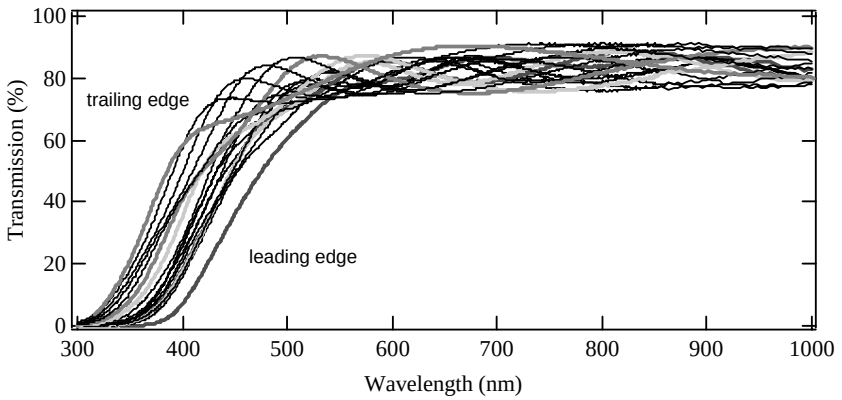

Fig. 5. The transmittance values of CTO62 (with substrate glass) are about 80%. Notice that the film optical absorption edges vary from around 400 nm at the leading edge to 350 nm at the trailing edge of the substrate.

4. Conclusion

SnO_2 and CdO thin films with high optical and electronic properties were made by MOCVD. Further, a linear combinatorial synthesis by combining both precursors for making SnO_2 and CdO film was used to fabricate Cd–Sn–O compounds. This high-throughput synthesis technique allows us to fabricate Cd–Sn–O compounds over a wide range of composition in a short time period. Large quantities of samples were formed and numerical characterization performed. Along with the compositional variation, the structure, electrical, and optical properties of the film all varied in a wide range. A high Hall mobility (50–60 $cm^2\ V^{-1}\ s^{-1}$) and reasonable carrier concentration ($10^{20}\ cm^{-3}$) were achieved in a wide Cd-to-Sn ratio. This result may point out a potential use for amorphous TCO materials. We believe that linear combinatorial synthesis has led to an increased understanding of the Cd–Sn–O system. Our findings provide guidance toward fabricating large-area, high-quality Cd_2SnO_4 by CVD.

Acknowledgements

Thanks to Mathew Young for EPMA characterization and Will Pratt, my summer intern, for optical characterization. This work was supported by the US Department of Energy under Contract No. DE-AC36-99GO10337.

References

[1] B.G. Lewis, D.C. Paine, MRS Bull. 25 (2000) 22.
[2] R.J. Hill, S.J. Nadel, Coated Glass Applications and Markets, Published by BOC Coating Technology, 2700 Maxwell Way, P.O. Box 2529, Fairfield, CA 94533-0252, ISBN #:0-914289-01-2.
[3] A.J. Nozik, Phys. Rev. 6 (2) (1972) 453.
[4] G. Haacke, H. Ando, W.E. Mealmaker, J. Electrochem. Soc. 124 (1977) 1923.
[5] C.M. Lambert, Solar Energy Mat. 6 (1981) 1.
[6] F. Golestani-Fard, F. Moztarzadeh, T. Hashemi, R. Nani, J. Aust. Ceram. Soc. 23 (1987) 86.
[7] G.N. Advani, A.G. Gordon, J. Electron. Mater. 9 (1980) 29.
[8] K. Gurumurugan, D. Mangalaraj, S.K. Narayandass, J. Electron. Mater. 25 (1996) 765–770.
[9] T.K. Subramanyam, S. Uthanna, B. Srinivasulu Naidu, Mater. Lett. 35 (1998) 214.
[10] A.A. Al-Quraini, C.H. Champness, in: Proceedings of the 26th PVSC Proc., Sept. 30–Oct. 3, 1997; Anaheim, CA, p. 415.
[11] K. Gurumurugan, J. Cryst. Growth 147 (1995) 355.
[12] N. Benramdane, W.A. Murad, R.H. Misho, M. Ziane, Z. Kebbab, Mater. Chem. Phys. 48 (1997) 119.
[13] G. Phatak, R. Lal, Thin Solid Films 245 (1994) 17.
[14] F.C. Eze, IL Nuovo Cimento 20 (1998) 1421.
[15] X. Li, D. Young, H. Moutinho, Y. Yang, C. Narayanswamy, R. Dhere, T.A. Gessert, T.J. Coutts, Electrochem. Solid State Lett. 4 (6) (2001) C43.
[16] X. Li, Y. Yan, T.A. Gessert, T.J. Coutts, Electrochem. Solid-State Lett. 4 (9) (2001) C66.
[17] T.M. Barnes, X. Li, C. DeHart, H. Moutinho, S. Asher, Y. Yan, T.A. Gessert, Mat. Res. Soc. Symp. Proc., 666 (2001) F1.8.7–F1.8.6.
[18] G. Haacke, Ann. Rev. Mater. Sci. 7 (1977) 73.
[19] T.J. Coutts, X. Wu, W.P. Mulligan, J.M. Webb, J. Electron. Mater. 25 (1996) 935.